

hUC-MSCs secreted exosomes inhibit the glioma cell progression through PTENP1/miR-10a-5p/PTEN pathway

S.-C. HAO^{1,2}, H. MA², Z.-F. NIU², S.-Y. SUN², Y.-R. ZOU², H.-C. XIA²

¹Ningxia Medical University, Yinchuan, China

²Department of Neurosurgery, The General Hospital of Ningxia Medical University, Yinchuan, China

Abstract. – OBJECTIVE: The mesenchymal stem cells (MSCs) have been widely studied for their anti-tumor property, due to the characteristic of homing towards tumor sites and immunosuppression. Nevertheless, the underlying molecular mechanisms that link MSCs to the targeted tumor cells, such as glioma, are not clear.

MATERIALS AND METHODS: Here, we examined the inhibitory properties and new molecular mechanisms of the human umbilical cord (hUC-MSCs) derived exosomes on the human glioma U87 cells using a co-culture system *in vitro*. The cell counting kit-8 (CCK-8) assay was performed to measure the anti-tumor activity of hUC-MSCs derived exosomes. The cell apoptosis was assessed by flow cytometry and the immunoblotting assay was applied in order to assess the associated proteins level. The data revealed that hUC-MSCs derived exosomes could repress cell proliferation and induce cell apoptosis.

RESULTS: Mechanistically, we identified that lncRNA PTENP1 could be packaged into exosome from hUC-MSCs, transferred to U87 cells, and then stabilized PTEN by binding miR-10a-5p competitively.

CONCLUSIONS: Therefore, our data suggested that the exosomes from hUC-MSCs possess a higher anti-tumor capacity, at least partially, via regulating miR-10a-5p/PTEN signaling, which thereby may represent a possible target for early diagnosis and treatment of glioma clinically.

Key Words:

hUC-MSCs, lncRNA PTENP1, miR-10a-5p, Glioma.

Introduction

Glioma is one of the most usual malignant brain tumors worldwide, despite the great improvements in early diagnosis and surgical techniques, as well as adjuvant radio-therapies and chemo-therapies^{1,2}. There are no curative treatments

for this kind of cancer, thus the prognosis of glioma patients is still poor and the mortality remains high. Although the immune therapeutic effect for glioma is making great progression, the war is further challenging. Therefore, it is urgently needed to understand the fully molecular mechanism of carcinogenesis and develop more novel and effective strategies for glioma.

The stem cell-based therapy containing the application of the induced pluripotent stem cells (iPSCs), neural stem cells (NSCs), and mesenchymal stem cells (MSCs) has been promisingly used to treat various diseases such as stroke, spinal cord injury, idiopathic pulmonary fibrosis, liver diseases, and malignant glioma³⁻⁷. The human mesenchymal stem cells (hMSCs) act as multipotent stem cells that could differentiate into different kinds of stromal cells under certain conditions. Besides, hMSCs are usually a key component in the microenvironment of the kinds of tumors, providing the potential application for cancer therapy⁸. Nevertheless, the data about the effect of hMSCs on the tumor features are contentious. Khakoo et al⁹ reported that hMSCs could inhibit the growth of tumor cells in Kaposi's sarcoma model, while Yu et al¹⁰ showed that hMSCs could promote the proliferative and invasive properties of osteosarcoma cells via *in vitro* co-culture model. The opposite results may be due in part to the different study systems and tumor types. Therefore, the potential effects of hMSCs on glioma cells need further investigation, which will benefit their use for clinical cancer therapy.

hMSCs are commonly derived from two sources including umbilical cord and bone marrow, named hUC-MSCs and hBM-MSCs accordingly^{11,12}. Previously, Lu et al¹³ explored the inhibited functions of hBM-MSCs on glioma U251 cells via affecting the PI3K/AKT signaling pathway. However, the effects and functional style of hUC-MSCs on glioma cells remain unclear. hM-

SCs-derived extracellular vesicles (EVs), mainly exosomes, are recently being assessed for their function in hMSCs-based cellular therapy. The exosomes, which contain various lncRNA and protein contents, participate in the communication and cell signaling between the cells. Therefore, we managed to evaluate the special effects and novel mechanisms of hUC-MSCs and their derived exosomes on glioma U87 cells via co-culture model.

In the present study, we established that the exosomes derived from hUC-MSCs could suppress the proliferation and promote the apoptosis of U87 cells. Mechanically, we identified that lncRNA PTENP1 in hUC-MSCs could be packaged into exosomes and transferred to U87 cells and relieved the suppressive effect of miR-10a-5p on the tumor suppressor gene PTEN, thus impairing the growth of glioma cells. In addition, the lncRNA PTENP1 level was decreased in tumor samples as compared with normal tissues, and was significantly associated with overall survival. All the data implied that the exosomal lncRNA PTENP1 might be a promising therapeutic target for clinical treatment in glioma.

Materials and Methods

Cell Lines and Culture

The human glioma cell line U87 was obtained from the Cell Bank of Chinese Academy of Science (Shanghai, China), and was cultured in Dulbecco's Modified Eagle's Medium (DMEM; Gibco, Rockville, MD, USA) added with 10% fetal bovine serum (FBS; Invitrogen, Carlsbad, CA, USA) and 1% penicillin-streptomycin (HyClone, South Logan, UT, USA) at 37°C with 5% CO₂.

hUC-MSCs Isolation and Culture Method

hUC-MSCs were isolated and cultured as previously described^{14,15}. Briefly, after the cesarean sections, the human umbilical cords were then collected from full-term healthy infants. Informed consent was obtained according to the institutional guidelines. The human umbilical cord was cut into 3-5 cm long segments, and the cord was washed with Phosphate-Buffered Saline (PBS) to remove blood as much as possible. The blood vessels containing two arteries and one vein were removed and the Wharton's jelly was retained. The retained Wharton's jelly was cut into pieces with 1 mm³ and then both pieces were grown in culture MEM medium, supplied with 10% FBS, 1% pen-

icillin-streptomycin, and basic fibroblast growth factor (10 ng/mL) in a humidified atmosphere at 37°C with 5% CO₂. After 1 week, the cells were adherent. hUC-MSCs displayed robust expression of the main MSC markers CD44 and CD105 by immunophenotypic analysis. hUC-MSCs could differentiate into adipogenic and osteogenic lineages when tested for differentiation capabilities, which suggested that hUC-MSCs are multipotent¹⁶. At 80-90% confluence, the cells were detached and reseeded for the experiments up to a maximum of 8 passages.

Exosomes Purification and Co-Culture

The exosomes were isolated from cultured hUC-MSCs using ExoQuick™ solution according to the manufacturer's protocol (System Biosciences, Palo Alto, CA, USA). Briefly, we collected the hUC-MSCs culture medium and centrifuged at 2800 g for 10 min in order to remove the cellular debris. Then, the supernatant was transferred to a new tube and the exosomes were precipitated using ExoQuick™ solution at 4°C on rotations overnight. Next day the pelleted exosomes were centrifuged from the mixture at 4°C for 30 min at 1500 g, followed by washing and re-suspending in PBS. The exosomes were stored at -80°C for a long time. The Bradford protein assay (Bio-Rad, Hercules, CA, USA) was applied to analyze the protein concentration of the isolated exosomes.

U87 cells were incubated with the exosomes in the serum-free medium at 37°C for 72 h. Then, the cells were collected and further analyzed.

Cell Transfection

The miR-10a-5p mimic and/or inhibitor, as well as the matching control, were obtained from RiboBio Co. (Guangzhou, China). The miR-10a-5p mimic/inhibitor or the matching control (150 nM) were transiently transfected into U87 cells using RNAi Max (Invitrogen, Carlsbad, CA, USA). The cells were collected and treated after 48 h transfection. The sequences were as follows: miR-10a-5p mimic: UACCCUGUAGAUCGAAUUUGUG; miR-10a-5p inhibitor: CACAAUUCGGAUCUACAGGGUA; Scramble: UUCUCCGAACGUGUCACGUUU.

To overexpress PTENP1, the vector, and the pCDNA3.1-PTENP1 plasmids were transfected into the U87 cells in the serum-free medium with Lipofectamine 2000™ (Invitrogen, Carlsbad, CA, USA) according to manufacturer's instructions. The medium in each well was changed with DMEM containing 10% heat-inactivated fe-

tal bovine serum after incubation at 37°C for 6 h. The cells were collected and treated after 48 h of transfection.

RNA Isolation and Quantitative Real Time-PCR (qRT-PCR)

MiRNAs extraction was performed by a miRNA Extraction Kit obtained from Tiangen (Beijing, China). After adding the Poly (A) firstly, 1 µg RNA including miRNAs was then reversely transcribed into complementary deoxyribose nucleic acid (cDNA). To detect the level of all miRNAs, we got the primers of the candidate miRNA and U6 from Sangon Biotech Co. (Shanghai, China). Moreover, the total RNA was isolated using TRIzol (Invitrogen, Carlsbad, CA, USA). Then, the total RNA was reversely transcribed into cDNA by a Promega reverse transcription kit (Madison, WI, USA) for the detection of lncRNA PTENP1 expression. The expression level of miRNA or PTENP1 was analyzed using SYBR Premix Ex Taq from TaKaRa (Dalian, China) in an ABI QS6 system (ABI, Applied Biosystems, Foster City, CA, USA). The endogenous control was U6 or glyceraldehyde 3-phosphate dehydrogenase (GAPDH). The qRT-PCR primers were as follows: PTENP1-F 5-TCAGAACATGG-CATACACCAA-3, PTENP1-R 5-TGATGAC-GTCCGATTTTCA-3; GAPDH-F 5-GGTG-GTCTCCTCTGACTTCAACA-3, and GAPDH-R 5-GTTGCTGTAGCCAAATTCGTTGT-3.

Immunoblotting Analysis

The cells were collected after co-culture or transfection. The total protein was extracted in 2X sodium dodecyl sulphate (SDS) sample buffer (4% SDS, 10% Glycine, 10 mM EDTA, 100 mM Tris-HCl (pH 6.8)). The primary antibodies to Bax, Cleaved caspase-3, Cyclin B1, Cyclin D1, PTEN, and GAPDH were obtained from Cell Signaling Technology (Danvers, MA, USA). The secondary antibodies containing anti-rabbit horseradish peroxidase (HRP) and anti-mouse HRP were obtained from Santa Cruz Biotechnology (Santa Cruz, CA, USA).

Cell Counting Kit-8 (CCK-8)

Viability Assay

The CCK-8 assay (Sigma-Aldrich, St. Louis, MO, USA) was performed to assess the growth of U87 cells. An equal number of cells was planted in 96-wells plate after transfection. After being cultured for various durations (12, 24, 48, and 72 h), the CCK-8 reagent was added to the cell

culture medium and incubated for another 1 h at 37°C. The 450 nm absorbance was then quantitatively measured.

Flow Cytometric Apoptosis Analysis

After co-culture or transfection, the U87 cells (250,000 cells/dish) were planted in 10 cm dishes. The cells were harvested later (at a cell confluency of 80%), washed in PBS, and stained with Annexin V and Propidium Iodide (PI; BD Biosciences, Detroit, MI, USA) for 30 min. The collected samples were subsequently evaluated using a Flow Cytometer (FACSCalibur; BD Biosciences, Detroit, MI, USA).

Dual-Luciferase Reporter Assays

The wild-type (WT) or mutated (MUT) lncRNA PTENP1 sequence including the potential binding sites of miR-10a-5p, as well as PTEN 3'-untranslated region (3'-UTR), were amplified via PCR and cloned into the pmrGLO vector (Promega, Madison, WI, USA). A mixture of 20 ng plasmids and 150 nM miR-10a-5p mimic were together transiently introduced into U87 cells. After transfection for 48 h, the firefly luciferase activity and the relative Renilla expression were measured using the Dual-Luciferase Reporter Assay System (Promega, Madison, WI, USA)

Statistical Analysis

All the results were presented as mean ± standard deviation (SD). We performed the statistical analysis using the Prism 6 (GraphPad Software, La Jolla, CA, USA), and the differences between different groups were estimated by the Student's *t*-test or Wilcoxon test. The overall survival (OS) rates were calculated using the Kaplan-Meier method, and then the log-rank test was applied for comparison. We considered it was statistically significant when a *p*-value < 0.05.

Results

The Purification and Identification of Isolated hUC-MSCs

hUC-MSCs were isolated and cultured according to the protocol and the cells were attached after 1 day of culture (Figure 1A). After passaged for 5 times, the cells displayed an evident lengthened morphology (Figure 1A). We then performed the immunophenotypic analysis to identify the surface marker of hUC-MSCs and found that the cultured hUC-MSCs exhibited a strong expression

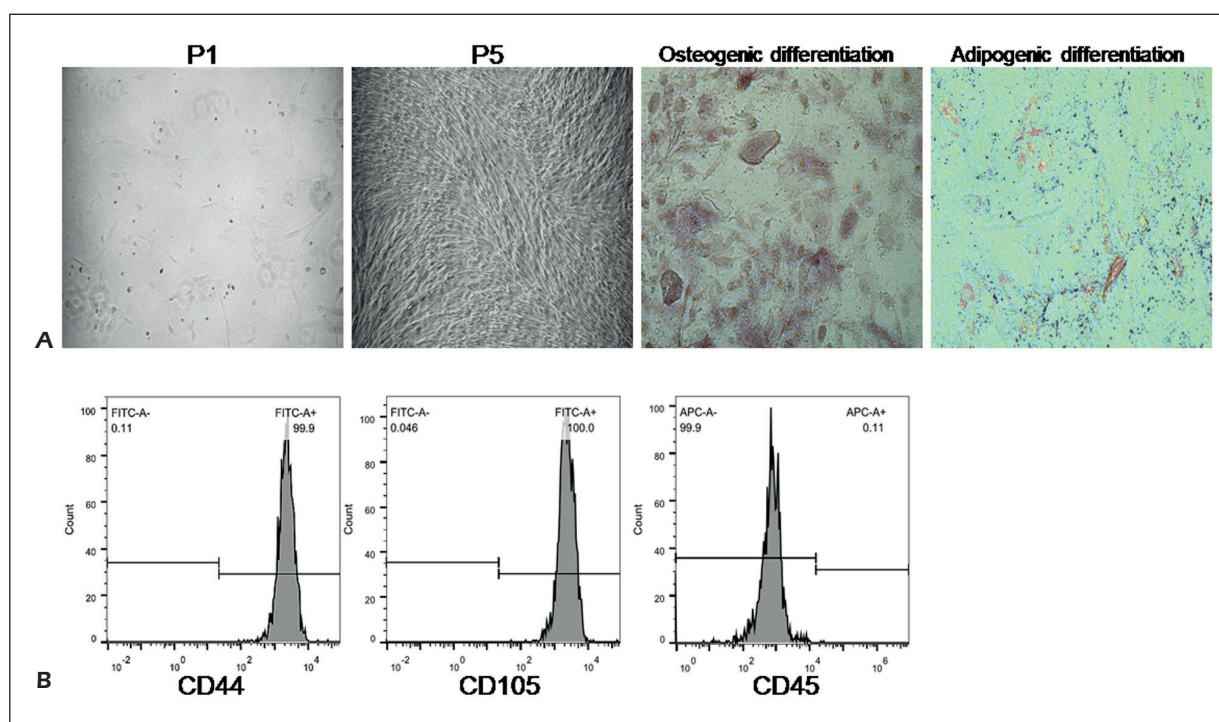


Figure 1. The purification and identification of hUC-MSCs. **A**, Morphology of primary hUC-MSCs after culturing for 1 (magnification: 100 \times) and 5 days (magnification: 100 \times), respectively. The Alizarin red staining (magnification: 200 \times) and oil red staining (magnification: 200 \times) results demonstrated osteogenesis differentiation and lipid differentiation, respectively. **B**, Positive antigen CD44 and CD105, as well as the negative antigen CD45, of isolated hUC-MSCs were identified by flow cytometry.

of the positive antigen CD44 and CD105, but not the negative antigen CD45 (Figure 1B), suggesting that the isolation of hUC-MSCs is successful. hUC-MSCs were considered to possess multipotent capacities to differentiate into adipogenic and osteogenic lineages. Subsequently, the Alizarin red staining and oil red staining were performed to test the differentiation capabilities. As expected, the data demonstrated that hUC-MSCs can differentiate into osteogenic and adipogenic lineages (Figure 1A), which suggested that the hUC-MSCs that we isolated are multipotent and could be applied for the following experiments.

Co-Culture of hUC-MSCs-Derived Exosomes Inhibits the Proliferation and Promotes the Apoptosis of U87 Cells

In order to investigate the function of hUC-MSCs-derived exosomes on glioma cells, we isolated the exosomes from hUC-MSCs and added them into the culture medium of U87 cells for a different time. The cell viability was then detected by the CCK-8 assay. The results showed that,

compared to the control group, the viability of U87 cells was remarkably decreased after treated with hUC-MSCs derived exosomes for 48 h and 72 h (Figure 2A). Consistent with attenuated cell growth, the protein level of the cell cycle-related molecules, including Cyclin B1, and Cyclin D1, were remarkably reduced after treated with hUC-MSCs derived exosomes (Figure 2B). Moreover, the flow cytometry data revealed that the apoptosis was significantly increased when challenged with hUC-MSCs derived exosomes (Figure 2C). Besides, the cleaved caspase-3, another marker of apoptosis, as well as apoptosis-related protein Bax, were also increased after hUC-MSCs derived exosomes treatment by immunoblotting assay (Figure 2D). Intriguingly, we found that the regulation of hUC-MSCs derived exosomes on these genes expression including *Cyclin B1*, *Cyclin D1*, *Bax*, and *Bcl-2* were dosage-dependent (Figure 2E, 2F), which further verifies the specificity of exosomes. In summary, the data proved that the co-culture of hUC-MSCs derived exosomes could suppress the proliferation and promote the apoptosis of the U87 cells.

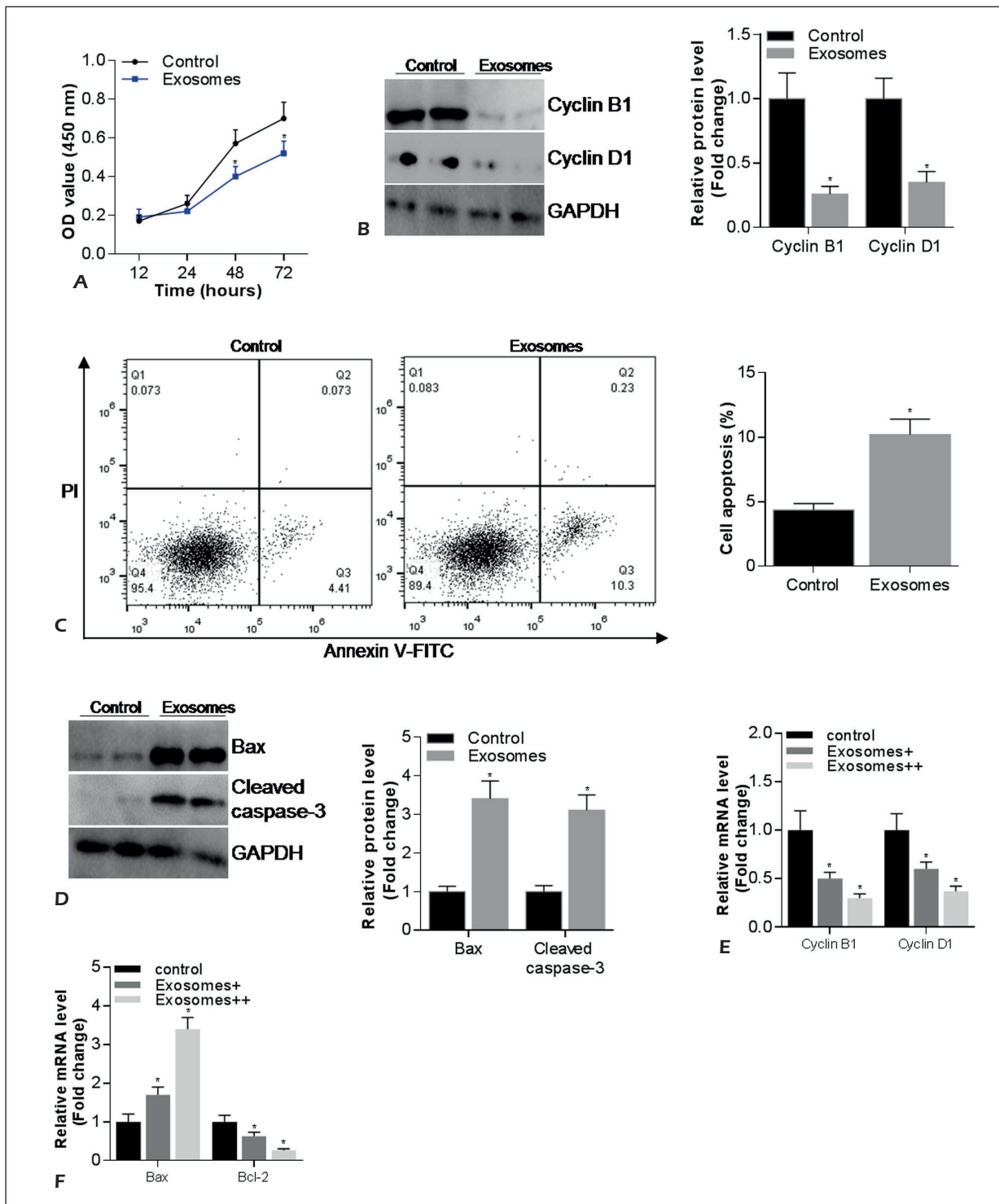


Figure 2. Co-culture of hUC-MSCs derived exosomes inhibits the proliferation and promotes the apoptosis of U87 cells. **A**, The viability of U87 cells treated with hUCMSCs-derived exosomes was analyzed by CCK-8 assay at the indicated time. **B**, The protein level of Cyclin B1 and Cyclin D1 in U87 cells were detected by Western blotting after the co-culture of hUC-MSCs derived exosomes. The protein level of GAPDH was used as the loading control. **C**, The apoptotic cells ratio was quantified by staining with PI and Annexin V-FITC using flow cytometry after treatment with hUCMSCs-derived exosomes. **D**, The expression of Bax and Cleaved caspase-3 in U87 cells was detected through Western blotting. The protein level of GAPDH was used as the loading control. **E**, The mRNA level of Cyclin B1 and Cyclin D1 in U87 cells were detected by qRT-PCR after the co-culture of hUC-MSCs derived exosomes with different concentration. **F**, The mRNA level of Bax and Bcl-2 in U87 cells were detected by qRT-PCR after the co-culture of hUC-MSCs derived exosomes with different concentration. $N \geq 3$, results shown as the mean \pm SD. * $p < 0.05$.

Exosomes-Mediated Transfer of LncRNA PTENP1 Caused the Decreased Cell Growth

It is reported that the lncRNA PTENP1 acts as the tumor suppressor gene by stabilizing PTEN in various cancer types¹⁷⁻¹⁹; however, the function of lncRNA PTENP1 in glioma remains to be determined. Thus, we first detected the expression of lncRNA PTENP1 in U87 cells after treatment of hUC-MSCs derived exosomes by qRT-PCR assay. Of note, we found that lncRNA PTENP1 was increased after the treatment of hUC-MSCs derived exosomes (Figure 3A). Moreover, we found that the expression of lncRNA PTENP1 was apparently lower in tumor samples than that in normal tissues (Figures 3B, 3C). We further performed the Kaplan-Meier survival analysis and the log-rank tests to evaluate the clinical significance of lncRNA PTENP1 in the prognosis of glioma patients. The data demonstrated that an increased level of lncRNA PTENP1 was associated with better overall survival in glioma (Figure 3D). To confirm that lncRNA PTENP1 can be packaged into exosomes, we overexpressed lncRNA PTENP1 in hUC-MSCs (Figure 3E); we found that lncRNA PTENP1 level in exosomes was indeed augmented in a dosage-dependent manner (Figure 3F). All the data implied the possible role of lncRNA PTENP1 in glioma.

To better explore the function of lncRNA PTENP1 in glioma, we overexpressed lncRNA PTENP1 in U87 cells (Figure 3G). We found that the lncRNA PTENP1 overexpression significantly decreased the proliferation of U87 cells in all examined time points using the CCK-8 assay (Figure 3H), indicating that lncRNA PTENP1 exerts a key role in the inhibition of the proliferation of U87 cells. Consistent with this phenotype, the protein level of Cyclin B1 and Cyclin D1 were also decreased after lncRNA PTENP1 overexpression (Figure 3I). We further applied flow cytometry to assess the effect of lncRNA PTENP1 on apoptosis. As expected, the number of apoptotic cells significantly increased after lncRNA PTENP1 overexpression (Figure 3J), indicating that lncRNA PTENP1 exerts an anti-apoptotic effect. The Bax and cleaved caspase-3 level both showed a significant upregulation trend when overexpressed with lncRNA PTENP1 (Figure 3K). Collectively, all the above data demonstrated that lncRNA PTENP1 transferred from exosomes mediated the decreased glioma cells growth.

LncRNA PTENP1 Affected Cell Growth by Targeting MiR-10a-5p in U87 Cells

It has been demonstrated that lncRNAs usually function as miRNA sponges, thereby tightly regulating the binding of endogenous miRNAs to their target mRNAs²⁰. We predicted by bioinformatic tools that miRNAs is a potential binding to lncBRM. Among these miRNA candidates, we noticed five important miRNA, miR-10a-5p, miR-107, miR-let-7a-5p, miR-619-5p, and miR-6720-5p, which are predicted to directly target PTEN using TargetScan software. MiR-10a-5p was selected, as it was largely decreased after lncRNA PTENP1 overexpression (Figure 4A). The Kaplan-Meier survival analysis displayed that lower miR-10a-5p level predicted better overall survival in glioma (Figure 4B). Further analyses exhibited that miR-10a-5p level in glioma tissues was dramatically higher than those observed in the paired adjacent healthy tissues (Figure 4C), suggesting the oncogenic role of miR-10a-5p in glioma.

To further determine the role of miR-10a-5p in glioma, the U87 cells were transfected with a particular miR-10a-5p inhibitor to decrease the level of miR-10a-5p than the control group (Figure 4D). CCK-8 assay displayed that miR-10a-5p deficiency in U87 cells leads to reduction of the cell growth (Figure 4E). The flow cytometry assay showed that, compared to the control group, the miR-10a-5p inhibitor treatment remarkably increased the cell apoptosis (Figures 4F-4G), also as reflected by increased cleaved caspase-3 and Bax (Figure 4H). The protein levels of Cyclin B1 and Cyclin D1 were also reduced after miR-10a-5p inhibitor treatment (Figure 4H). These analyses consistently suggested that lncRNA PTENP1 might affect cell growth by targeting the oncogenic miR-10a-5p in U87 cells.

LncRNA PTENP1/MiR-10a-5p/PTEN Cascades Contributed to the U87 Cell Growth

In order to further elucidate the molecular mechanism, we next cloned wild-type (WT) lncRNA PTENP1 luciferase plasmids containing potential miR-10a-5p binding sites or mutants (MUT) for each site. Then, the luciferase assays were performed to confirm whether miR-10a-5p interacts with lncRNA PTENP1 after co-transfecting these plasmids with miR-10a-5p mimics and miR-10a-5p inhibitor into U87 cells. As Figures 5A-5B shown, miR-10a-5p mimics substantially inhibited, while miR-10a-5p inhibitor

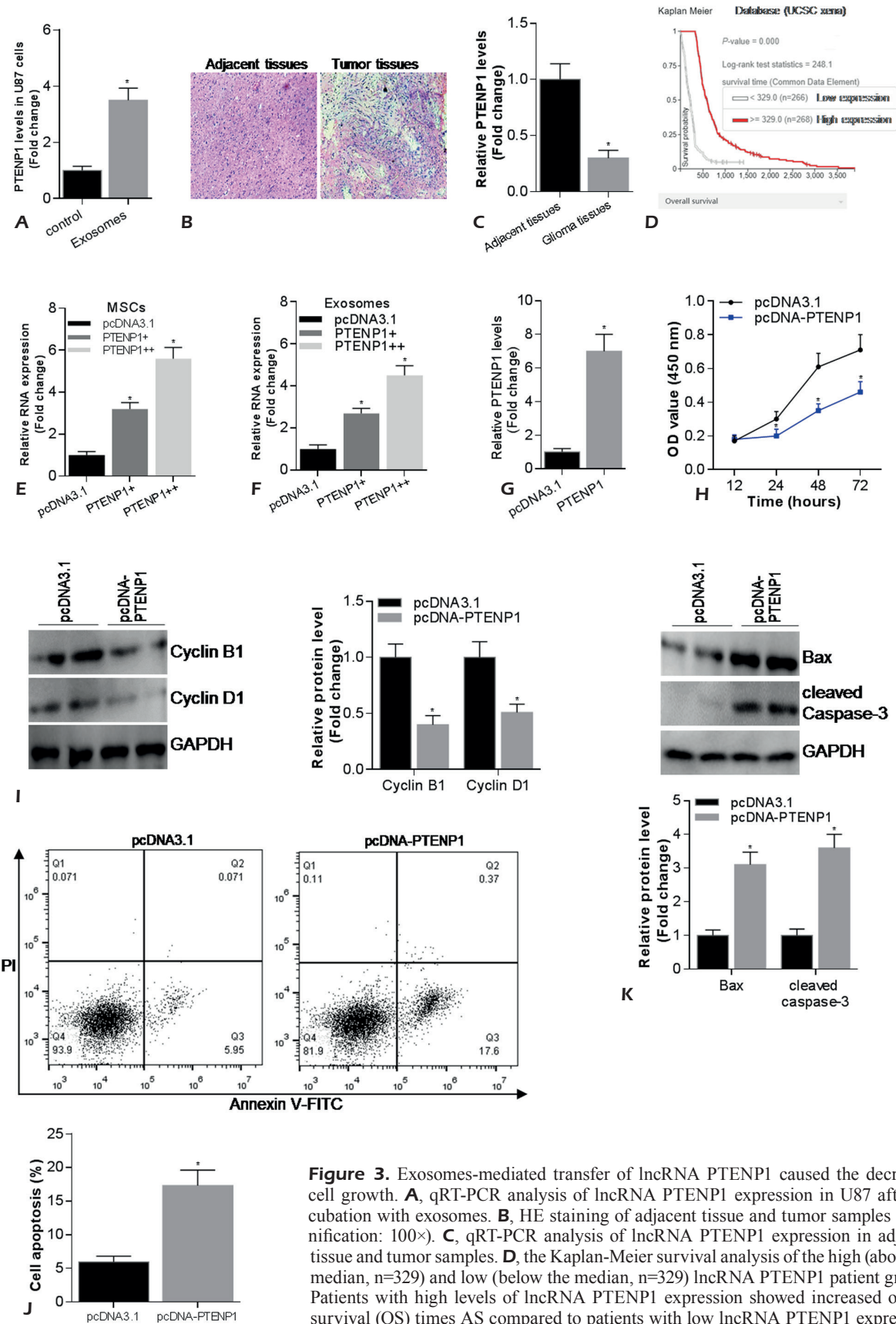


Figure 3. Exosomes-mediated transfer of lncRNA PTENP1 caused the decreased cell growth. **A**, qRT-PCR analysis of lncRNA PTENP1 expression in U87 after incubation with exosomes. **B**, HE staining of adjacent tissue and tumor samples (magnification: 100×). **C**, qRT-PCR analysis of lncRNA PTENP1 expression in adjacent tissue and tumor samples. **D**, the Kaplan-Meier survival analysis of the high (above the median, n=329) and low (below the median, n=329) lncRNA PTENP1 patient groups. Patients with high levels of lncRNA PTENP1 expression showed increased overall survival (OS) times AS compared to patients with low lncRNA PTENP1 expression. **E**, Confirm of lncRNA PTENP1 expression in hUC-MSCs by qRT-PCR analysis after overexpression. **F**, qRT-PCR analysis of lncRNA PTENP1 expression in exosomes that were derived from hUC-MSCs. **G**, lncRNA PTENP1 expression in U87 cells was analyzed by qRT-PCR analysis. **H**, The viability of U87 cells after lncRNA PTENP1 overexpression was analyzed by CCK-8 assay. **I**, The protein level of Cyclin B1 and Cyclin D1 in U87 cells were detected by Western blotting. The protein level of GAPDH was used as the loading control. **J**, The apoptotic cells ratio was quantified by double-supravital staining with PI and Annexin V-FITC using flow cytometry. **K**, Western blotting was performed to detect the expression of Bax and Cleaved caspase-3 in U87 cells. The protein level of GAPDH was used as the loading control. N ≥ 3, results shown as the mean ± SD. *p<0.05.

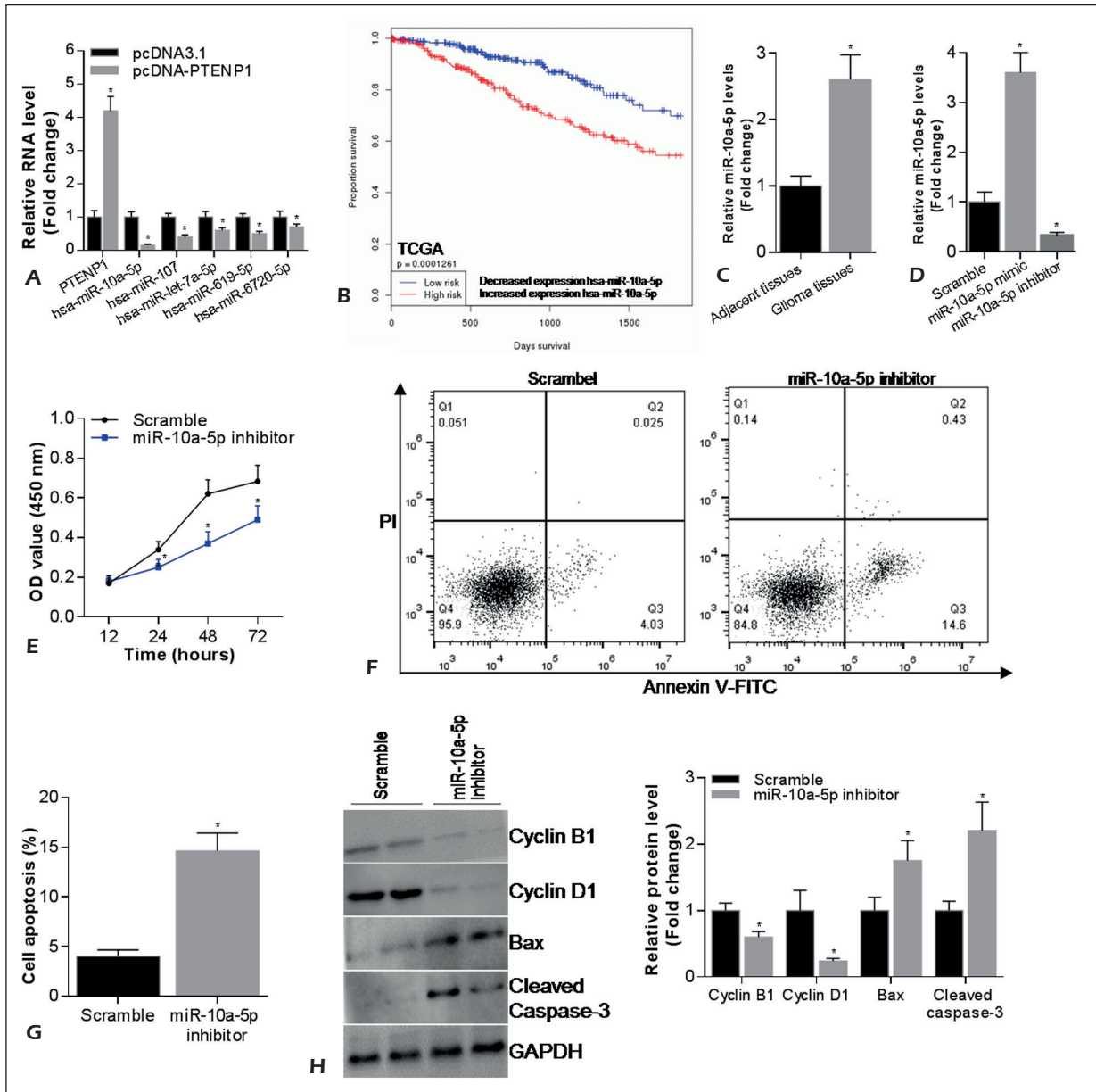


Figure 4. LncRNA PTENP1 affected the cell growth by targeting miR-10a-5p in U87 cells. **A**, qRT-PCR analysis of lncRNA PTENP1, miR-10a-5p, miR-107, miR-let-7a-5p, miR-619-5p, and miR-6720-5p expression in U87 after lncRNA PTENP1 over-expression. **B**, The Kaplan-Meier survival analysis of the high and low miR-10a-5p patient groups in TCGA database. **C**, qRT-PCR analysis of miR-10a-5p expression in adjacent tissue and glioma tumor samples. **D**, qRT-PCR analysis of miR-10a-5p expression after the treatment with miR-10a-5p inhibitor. **E**, The effect of miR-10a-5p on U87 cell growth was measured by CCK-8. U87 cells were treated with miR-10a-5p inhibitor. **F-G**, The effect of miR-10a-5p on U87 cell apoptosis were quantified by staining with Annexin V-FITC and PI using flow cytometry. **H**, The effect of miR-10a-5p on expressions of Cyclin B1, Cyclin D1, Bax, and Cleaved caspase-3 in U87 cells were evaluated by Western blotting. The protein level of GAPDH was used as the loading control. $N \geq 3$, results shown as the mean \pm SD. * $p < 0.05$.

increased the luciferase activity of WT lncRNA PTENP1. However, they failed to affect the luciferase activity of the lncRNA PTENP1 mutants, suggesting that miR-10a-5p directly bind lncRNA PTENP1 (Figures 5A-5B). We further confirmed the interaction by comparing the effect of the orig-

inal miR-10a-5p mimics or miR-10a-5p mutants with a mutation in potential lncRNA PTENP1 binding sites. Although the luciferase activity of the lncRNA PTENP1 was inhibited after transfection with miR-10a-5p mimics, it was unaffected by miR-10a-5p mutants (Figure 5C).

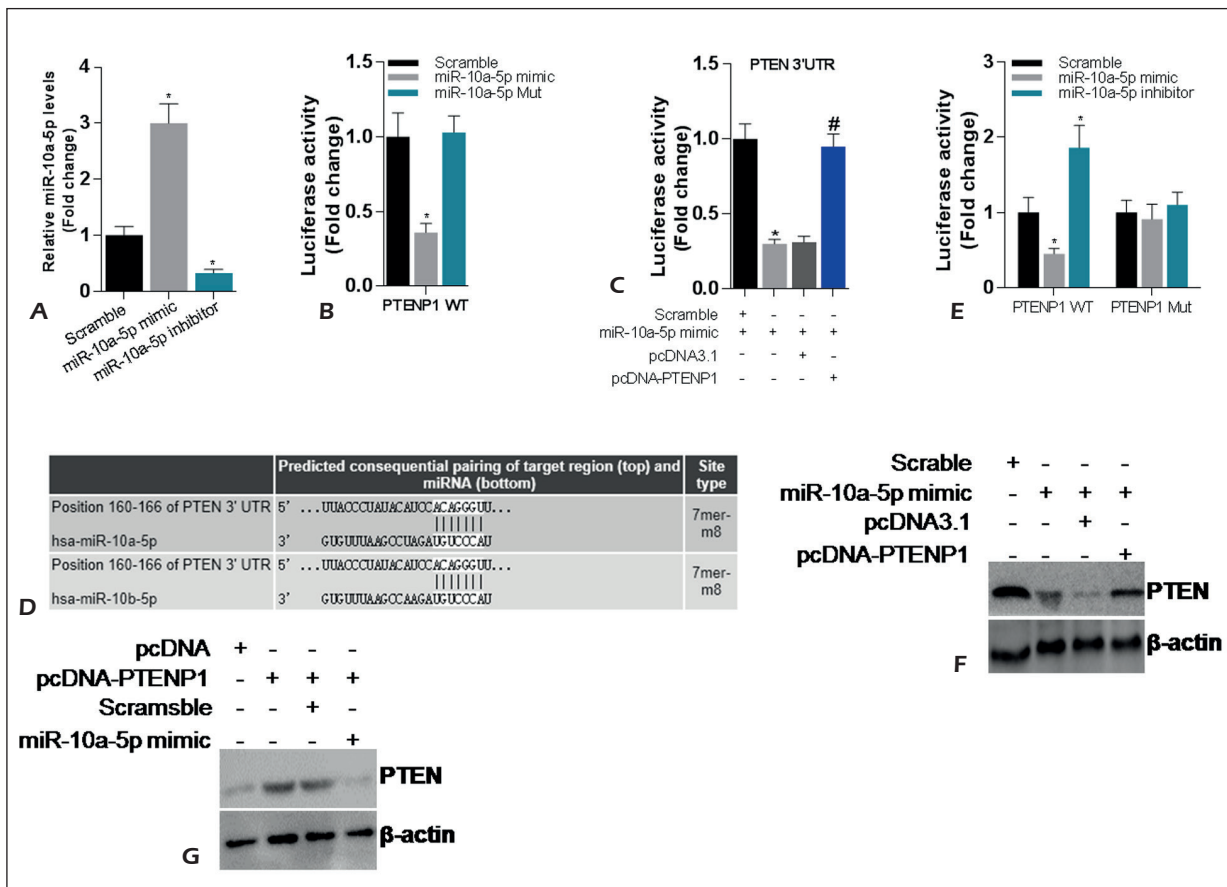


Figure 5. LncRNA PTENP1 affected the cell growth by targeting miR-10a-5p in U87 cells. **A**, qRT-PCR analysis of miR-10a-5p expression after treated with miR-10a-5p inhibitor and mimics. **B**, The effect of miR-10a-5p on the activity of luciferase reporter containing either wild-type (WT) or the mutated (Mut) lncRNA PTENP1 3'UTR was tested by the luciferase reporter gene assays. U87 cells were transfected with WT or the Mut PTENP1 3'UTR luciferase reporter plasmids and the miR-10a-5p mimic or inhibitor. **C**, The effect of wild-type (WT) or the mutated (Mut) miR-10a-5p on the activity of luciferase reporter containing lncRNA PTENP1 3'UTR was studied by the luciferase reporter gene assays. **D**, The sequence alignment between miR-10a-5p and the 3'-UTR of PTEN mRNA predicted by TargetScan. **E**, The causal effect of miR-10a-5p and lncRNA PTENP1 on the activity of the luciferase reporter containing PTEN 3'UTR was examined by the luciferase reporter gene assays. **F-G**, The effect of miR-10a-5p and lncRNA PTENP1 on the protein level of PTEN was evaluated through Western blotting. The protein level of GAPDH was used as the loading control. $N \geq 3$, results shown as the mean \pm SD. * $p < 0.05$.

We next wondered whether lncRNA PTENP1 regulated PTEN expression via interacting with miR-10a-5p due to the prediction by bioinformatics (Figure 5D). To test this hypothesis, the luciferase reporter vector containing PTEN 3'UTR was co-transfected with miR-10a-5p mimics into the U87 cells with or without lncRNA PTENP1. Likewise, miR-10a-5p mimics repressed the luciferase activity of PTEN 3'UTR, whereas lncRNA PTENP1 overexpression totally abolished these effects (Figure 5E). The protein level of PTEN was also impaired after miR-10a-5p mimics transfection, however, it was rescued by lncRNA PTENP1 overexpression (Figure 5F). Besides, we also found that lncRNA PTENP1 overexpres-

sion promoted the PTEN expression, which was abolished after miR-10a-5p mimics transfection (Figure 5G). In total, we identified that the exosome-derived lncRNA PTENP1 regulates the PTEN expression in glioma by competitively binding miR-10a-5p, suggesting the potential clinical application of targeting lncRNA PTENP1/miR-10a-5p/PTEN cascades in glioma.

Discussion

Glioma, one of the most common and lethal solid brain tumor, has a poor prognosis despite the great effect in conventional therapeutic ap-

proaches^{21,22}; thus, developing novel therapeutic strategies is extremely crucial. Recently, stem cell therapy for different kinds of cancer has been proposed and tested because of its evident advantages in many ways²³. The mesenchymal stem cells (MSCs) are a mesenchymal cell type that possesses strong self-renewal ability and multidirectional differentiation capacity²⁴. Previous studies have shown that MSCs could affect the behavior of cancer cells in a context-dependent manner, which may be due to diverse communication concerning MSCs and tumor cells. Thus, exploring the comprehensive effects of MSCs on glioma cells systematically, and dissecting the novel mechanism of such an effect are urgently needed.

In the present study, we investigated the repressive effects of hUC-MSCs derived exosomes in glioma U87 cells and elucidated the novel underlying molecular mechanisms. We first examined the effects of hUC-MSCs derived exosomes on U87 cells proliferation and apoptosis by co-culturing with U87 cells. Our data clearly exhibited that those hUC-MSCs derived exosomes could inhibit the proliferation and further promote the cell death of U87 cells *in vitro*. As well known, the cell cycle progress is finely controlled by the cell cycle regulatory proteins, involving Cyclins, Cyclin-dependent kinases (CDKs), and CDK inhibitors²⁵. Cyclin B1 and Cyclin D1 are essential to cell cycle regulatory proteins and the hUC-MSCs derived exosomes markedly downregulated Cyclin B1 and Cyclin D1 in U87 cells. Consistent with the augmented apoptosis, immunoblotting demonstrated that the cleaved caspase-3 that is triggered by pro-apoptotic molecules, such as cytochrome c releasing from mitochondria, as well as Bax, were remarkably increased after co-culturing with hUC-MSCs derived exosomes, which is consistent with the previous results²⁶.

The various types of cells could release exosomes into the extracellular microenvironment and the exosomes are tightly involved in intercellular communication through the cell contents (DNA, RNA, proteins, and lipids)²⁷. In this study, we showed that the transfer of exosomal lncRNA PTENP1 from MSCs to glioma cells inhibited the glioma cells growth by decreasing the ability to proliferate and increase apoptosis. These data led us to further investigate the molecular mechanism of putative tumor suppressor lncRNA PTENP1 in human glioma cells. Many studies^{17,18,28-30} reported that lncRNA PTENP1 could serve as a competing endogenous RNA (ceRNA) to bind miRNAs competitively, thus modulating

PTEN expression in several cancers. Thus, we performed a series of assays and found that lncRNA PTENP1 protected PTEN degradation by sponging miR-10a-5p, and suppressed the biological malignant behavior of glioma U87 cells. Besides, we firstly identified the oncogenic function of miR-10a-5p in glioma cells, as there have been few reports describing the function of miR-10a-5p. MiR-10a-5p was augmented in cancer tissues compared to normal tissue and lower miR-10a-5p levels predicted a better overall survival, raising the possibility of miR-10a-5p as a promising novel diagnostic biomarker for glioma. Whether miR-10a-5p participates in the migration and invasion of glioma remain to be determined in the future.

Conclusions

We demonstrated that hUC-MSCs could package lncRNA PTENP1 into exosomes, and then transfer it into glioma cells. That exogenous lncRNA PTENP1 may act as a miR-10a-5p decoy to regulate PTEN expression, and then suppress glioma cell viability, which suggested that the exosomal lncRNA PTENP1 could mediate the cell-cell communication and that hUC-MSCs derived exosomes may provide the alternative strategies for the treatment of glioma.

Conflict of Interests

The Authors declared that they have no conflict of interests.

References

- 1) BRAY F, FERLAY J, SOERJOMATARAM I, SIEGEL RL, TORRE LA, JEMAL A. Global cancer statistics 2018: GLOBOCAN estimates of incidence and mortality worldwide for 36 cancers in 185 countries. *CA Cancer J Clin* 2018; 68: 394-424.
- 2) LEFRANC F, SADEGHI N, CAMBY I, METENS T, DEWITTE O, KISS R. Present and potential future issues in glioblastoma treatment. *Expert Rev Anticancer Ther* 2006; 6: 719-732.
- 3) KOKAIA Z, DARSALIA V. Neural stem cell-based therapy for ischemic stroke. *Transl Stroke Res* 2011; 2: 272-278.
- 4) BEXELL D, SVENSSON A, BENZON J. Stem cell-based therapy for malignant glioma. *Cancer Treat Rev* 2013; 39: 358-365.
- 5) MUHEREMU A, PENG J, AO Q. Stem cell based therapies for spinal cord injury. *Tissue Cell* 2016; 48: 328-333.
- 6) BARCZYK M, SCHMIDT M, MATTOLI S. Stem cell-based therapy in idiopathic pulmonary fibrosis. *Stem Cell Rev* 2015; 11: 598-620.

- 7) SHIOTA G, ITABA N. Progress in stem cell-based therapy for liver disease. *Hepatol Res* 2017; 47: 127-141.
- 8) MOHAMMADPOUR H, POURFATHOLLAH AA, NIKOUGOFTAR ZM, SHAHBAZAFAR AA. Irradiation enhances susceptibility of tumor cells to the antitumor effects of TNF-alpha activated adipose derived mesenchymal stem cells in breast cancer model. *Sci Rep* 2016; 6: 28433.
- 9) KHAKOO AY, PATI S, ANDERSON SA, REID W, ELSHAL MF, ROMERA II, NGUYEN AT, MALIDE D, COMBS CA, HALL G, ZHANG J, RAFFELD M, ROGERS TB, STETLER-STEVENSON W, FRANK JA, REITZ M, FINKEL T. Human mesenchymal stem cells exert potent antitumorigenic effects in a model of Kaposi's sarcoma. *J Exp Med* 2006; 203: 1235-1247.
- 10) YU FX, HU WJ, HE B, ZHENG YH, ZHANG QY, CHEN L. Bone marrow mesenchymal stem cells promote osteosarcoma cell proliferation and invasion. *World J Surg Oncol* 2015; 13: 52.
- 11) QIAO C, XU W, ZHU W, HU J, QIAN H, YIN Q, JIANG R, YAN Y, MAO F, YANG H, WANG X, CHEN Y. Human mesenchymal stem cells isolated from the umbilical cord. *Cell Biol Int* 2008; 32: 8-15.
- 12) PITTENGER MF, MACKAY AM, BECK SC, JAISWAL RK, DOUGLAS R, MOSCA JD, MOORMAN MA, SIMONETTI DW, CRAIG S, MARSHAK DR. Multilineage potential of adult human mesenchymal stem cells. *Science* 1999; 284: 143-147.
- 13) LU L, CHEN G, YANG J, MA Z, YANG Y, HU Y, LU Y, CAO Z, WANG Y, WANG X. Bone marrow mesenchymal stem cells suppress growth and promote the apoptosis of glioma U251 cells through down-regulation of the PI3K/AKT signaling pathway. *Biomed Pharmacother* 2019; 112: 108625.
- 14) MA S, LIANG S, JIAO H, CHI L, SHI X, TIAN Y, YANG B, GUAN F. Human umbilical cord mesenchymal stem cells inhibit C6 glioma growth via secretion of dickkopf-1 (DKK1). *Mol Cell Biochem* 2014; 385: 277-286.
- 15) NAGAMURA-INOUE T, HE H. Umbilical cord-derived mesenchymal stem cells: Their advantages and potential clinical utility. *World J Stem Cells* 2014; 6: 195-202.
- 16) CAPELLI C, GOTTI E, MORIGI M, ROTA C, WENG L, DAZZI F, SPINELLI O, CAZZANIGA G, TREZZI R, GIANATTI A, RAMBALDI A, GOLAY J, INTRONA M. Minimally manipulated whole human umbilical cord is a rich source of clinical-grade human mesenchymal stromal cells expanded in human platelet lysate. *Cytotherapy* 2011; 13: 786-801.
- 17) ZHENG R, DU M, WANG X, XU W, LIANG J, WANG W, LV Q, QIN C, CHU H, WANG M, YUAN L, QIAN J, ZHANG Z. Exosome-transmitted long non-coding RNA PTENP1 suppresses bladder cancer progression. *Mol Cancer* 2018; 17: 143.
- 18) QIAN YY, LI K, LIU QY, LIU ZS. Long non-coding RNA PTENP1 interacts with miR-193a-3p to suppress cell migration and invasion through the PTEN pathway in hepatocellular carcinoma. *Oncotarget* 2017; 8: 107859-107869.
- 19) LI RK, GAO J, GUO LH, HUANG GQ, LUO WH. PTENP1 acts as a ceRNA to regulate PTEN by sponging miR-19b and explores the biological role of PTENP1 in breast cancer. *Cancer Gene Ther* 2017; 24: 309-315.
- 20) GUO T, LI J, ZHANG L, HOU W, WANG R, ZHANG J, GAO P. Multidimensional communication of microRNAs and long non-coding RNAs in lung cancer. *J Cancer Res Clin Oncol* 2019; 145: 31-48.
- 21) XU CH, XIAO LM, LIU Y, CHEN LK, ZHENG SY, ZENG EM, LI DH. The lncRNA HOXA11-AS promotes glioma cell growth and metastasis by targeting miR-130a-5p/HMGB2. *Eur Rev Med Pharmacol Sci* 2019; 23: 241-252.
- 22) WESTPHAL M, LAMSZUS K. The neurobiology of gliomas: from cell biology to the development of therapeutic approaches. *Nat Rev Neurosci* 2011; 12: 495-508.
- 23) REAGAN MR, SEIB FP, McMILLIN DW, SAGE EK, MITSIADES CS, JANES SM, GHOBRIAL IM, KAPLAN DL. Stem cell implants for cancer therapy: TRAIL-expressing mesenchymal stem cells target cancer cells in situ. *J Breast Cancer* 2012; 15: 273-282.
- 24) SUN DZ, ABELSON B, BABBAR P, DAMASER MS. Harnessing the mesenchymal stem cell secretome for regenerative urology. *Nat Rev Urol* 2019; 16: 363-375.
- 25) ROSKOSKI RJ. Cyclin-dependent protein kinase inhibitors including palbociclib as anticancer drugs. *Pharmacol Res* 2016; 107: 249-275.
- 26) WU HH, LEE OK. Exosomes from mesenchymal stem cells induce the conversion of hepatocytes into progenitor oval cells. *Stem Cell Res Ther* 2017; 8: 117.
- 27) BOELENS MC, WU TJ, NABET BY, XU B, QIU Y, YOON T, AZZAM DJ, TWYMAN-SAINT VC, WIEMANN BZ, ISHWARAN H, TER BRUGGE PJ, JONKERS J, SLINGERLAND J, MINN AJ. Exosome transfer from stromal to breast cancer cells regulates therapy resistance pathways. *Cell* 2014; 159: 499-513.
- 28) YU G, YAO W, GUMIREDDY K, LI A, WANG J, XIAO W, CHEN K, XIAO H, LI H, TANG K, YE Z, HUANG Q, XU H. Pseudogene PTENP1 functions as a competing endogenous RNA to suppress clear-cell renal cell carcinoma progression. *Mol Cancer Ther* 2014; 13: 3086-3097.
- 29) GAO L, REN W, ZHANG L, LI S, KONG X, ZHANG H, DONG J, CAI G, JIN C, ZHENG D, ZHI K. PTENp1, a natural sponge of miR-21, mediates PTEN expression to inhibit the proliferation of oral squamous cell carcinoma. *Mol Carcinog* 2017; 56: 1322-1334.
- 30) ZHANG R, GUO Y, MA Z, MA G, XUE Q, LI F, LIU L. Long non-coding RNA PTENP1 functions as a ceRNA to modulate PTEN level by decoying miR-106b and miR-93 in gastric cancer. *Oncotarget* 2017; 8: 26079-26089.